

Preparation of Bioactive Mesoporous Calcium Phosphate Granules

O. N. Musskaya^{a,*}, A. I. Kulak^a, V. K. Krut'ko^a, Yu. A. Lesnikovich^b,
V. V. Kazbanov^c, and N. S. Zhitkova^c

^a *Institute of General and Inorganic Chemistry, Belarusian Academy of Sciences, ul. Surganova 9/1, Minsk, 220072 Belarus*

^b *Belarussian State University, Leningradskaya ul. 14, Minsk, 220030 Belarus*

^c *Republican Scientific and Practical Centre for Pediatric Surgery, pr. Nezavisimosti 64, Minsk, 220013 Belarus*

*e-mail: musskaja@igic.bas-net.by

Received April 4, 2017; in final form, September 7, 2017

Abstract—Mesoporous calcium phosphate granules ranging in mesopore size from 11 to 19 nm have been prepared using cryogenic processing (–18°C) of gels and extrusion of calcium phosphate paste. The granules based on acid calcium phosphates have a relatively small specific surface area (45 m²/g) in comparison with the neutral and basic calcium phosphates (84–155 m²/g). Preclinical in vivo trials on rats show that the presence of calcium phosphate granules in a bone defect considerably accelerates reparative osteogenesis in comparison with a control group of animals.

Keywords: calcium phosphates, hydroxyapatite, tricalcium phosphate, specific surface area, bioactivity

DOI: 10.1134/S0020168518020115

INTRODUCTION

It is known that bone substitute materials should be nontoxic; capable of resorbing, being replaced by bone tissue; easy to sterilize; and convenient for use under clinical conditions and in a hospital environment. Analysis of the modern literature indicates that, currently, intrinsic bone tissue of patients is used more rarely for bone tissue regeneration because intrinsic bone extraction is a second painful intervention [1–6].

In recent years, ever increasing attention has been paid to synthetic materials, such as hydroxyapatite (HA) and tricalcium phosphate (TCP), whose crystals are subject to metabolism by cells in a biological medium and decompose into calcium and phosphate ions, which then enter into the structure of regenerated bone tissue. The key criteria in selecting synthetic materials are biocompatibility, high porosity, the ability to act as a matrix in the bone tissue regeneration process, and total or partial resorbability. The resorbability of a material depends on both the nature of the calcium phosphate and its porosity, which is a key factor in bone tissue regeneration. The presence of macropores, that is, spaces between granules stable to pressure, creates favorable conditions for bone formation and angiogenesis. High microporosity of calcium phosphates improves the osteoconductive properties of the material and increases the degree of regeneration of the new bone. The final result of the regeneration process is the integration of the new intrinsic bone

and HA. Integrated HA can ensure atrophy prevention and maintain the hard tissue volume for a long time.

Currently, calcium phosphate granules, in particular, Interpore®, ProOsteon®, Osteogen®, Tecknomed®, Osteograf/N®, BIO-OSS®, TricOs™, MBCP®, easy-graft®, and easy-graft®CRYSTAL [1–4], are widely used as effective, biocompatible bone defect fillers. They serve the function of matrices for cell cultures and substitute for bone defects. In addition, HA- and TCP-based granules are used as drug delivery systems for local therapy [5, 6].

The preparation of calcium phosphate granules is typically accompanied by the exposure of the calcium phosphates to high temperatures, which reduces the degree of their bioactivity in comparison with unheated calcium phosphates, which contain water of crystallization [7, 8].

In this paper, we report the preparation and physicochemical characterization of mesoporous calcium phosphate granules at room temperature and –18°C in their most biologically active, hydrated form.

EXPERIMENTAL

Calcium phosphates were synthesized by reacting aqueous calcium chloride and diammonium hydrogen phosphate solutions, while varying the pH of the reaction in the range 5–11 and the Ca/P ratio in the range 1.50–1.67 [9–12]. The resultant 3 to 5% calcium phosphate gel was further concentrated to a 28 to 31%

paste in a BiofugePrimo centrifuge (Germany) using a fixed-angle rotor (7500 rpm, 2 h).

Calcium phosphate granules were produced by two procedures: (1) cryogenic processing of the 3 to 5% calcium phosphate gels and (2) extrusion of the 28 to 31% calcium phosphate paste. In the former procedure, the calcium phosphate (brushite, monetite, TCP, and HA) gel was held at -18°C for 24 h and then dried in air (at 20°C).

In the latter procedure, the calcium phosphate paste was extruded through a sieve with an aperture size of 1.6 mm. The resultant moist granules were dehydrated in three ways: (1) by air-drying (at 20°C); (2) by cryogenic processing (at -18°C for 24 h), followed by air-drying (at 20°C); and (3) by treatment with a 30% hydrogen peroxide solution, followed by air-drying (at 20°C). In addition, the surface of the granules produced by the latter procedure was treated with a 5% HA suspension (aqueous or based on a 1% polyvinyl alcohol (PVA) solution) for 10 min using a water jet pump. The granule-to-HA suspension weight ratio was 1 : 20. After the treatment, the granules were air-dried at room temperature to constant weight.

The phase composition of the resultant materials was determined by X-ray diffraction on an Advance D8 diffractometer (Bruker, Germany) and a DRON-3 diffractometer (Russia) with $\text{CuK}\alpha$ radiation ($\lambda = 1.5405 \text{ \AA}$), using Match Version 2.1.1.1 database resources. The size of the calcium phosphate granules was analyzed using an MIN-8 polarized-light microscope (Russia). The surface morphology of the granules was examined on a LEO 1420 conventional scanning electron microscope (Germany).

The adsorption properties of the granules were studied using an ASAP 2020 MP surface area and porosity analyzer (the United States). The specific surface area was determined by BET analysis (A_{BET}). The adsorption and desorption cumulative pore surface area ($A_{\text{BJH ads}}$ and $A_{\text{BJH des}}$, respectively) and adsorption and desorption cumulative pore volume ($V_{\text{BJH ads}}$ and $V_{\text{BJH des}}$) at pore diameters from 1.7 to 300 nm were evaluated by the Barrett–Joyner–Halenda (BJH) method. The adsorption pore volume ($V_{\text{sp ads}}$) was determined by the t -method.

Preclinical trials were carried out on male Wistar rats. For in vitro trials, we used calcium phosphate granules having a large specific surface area and consisting of a few calcium phosphate phases. Implants were inserted in a premodeled defect in the parietal bone of all the rats under general anesthesia (urethane–pentobarbital, 0.2 mL/100 g of body weight), followed by operative wound closure. The animals were divided into three groups (five rats in each): (I) control group (with a false defect), (II) group having inserted titanium implants, and (III) group having

inserted titanium implants and calcium phosphate granules. Antimicrobial therapy was conducted with gemcitabine. Histology of bone tissue in contact with the implants was examined three months after the surgical intervention.

RESULTS AND DISCUSSION

The X-ray diffraction patterns of the calcium phosphates synthesized at $\text{Ca} : \text{P} = 1.5$ and pH 5–6 (Fig. 1a) and then dried at $60\text{--}70^{\circ}\text{C}$ show strong reflections from dicalcium phosphate in the form of brushite ($2\theta = 11.7^{\circ}$, 20.9° , and 29.3°), weaker reflections from dicalcium phosphate in the form of monetite ($2\theta = 26.5^{\circ}$ and 30.2°), and an X-ray amorphous halo at $2\theta = 25.6^{\circ}$ and 31.9° due to an amorphous calcium phosphate (ACP). Raising pH to 6–11 at $\text{Ca} : \text{P} = 1.5\text{--}1.67$ causes the reflections from the acid calcium phosphates to disappear.

Heat treatment of monetite and brushite at 800°C leads to the formation of tetracalcium phosphate ($\text{Ca}_4\text{P}_2\text{O}_9$) and the acid calcium pyrophosphate $\text{CaH}_2\text{P}_2\text{O}_7$ (Fig. 1b). Heat treatment of the ACP prepared at $\text{Ca} : \text{P} = 1.5$ in an acid medium (pH 5) or a neutral or weakly alkaline medium (pH 6–8) leads to complete β -TCP crystallization in the form of whitlockite ($2\theta = 25.9^{\circ}$, 31.7° , 32.2° , and 32.9°). Increasing the $\text{Ca} : \text{P}$ ratio to 1.67 at pH 8–9 leads to the crystallization of a two-phase material: HA + α -TCP (the reflections from the α -TCP are located at $2\theta = 22.7^{\circ}$, 30.8° , and 34.2°), whereas at pH 10–11 phase-pure HA crystallizes ($2\theta = 25.9^{\circ}$, 31.7° , 32.2° , and 32.9°).

The calcium phosphate granules produced by cryogenic processing of the 3 to 5% calcium phosphate gels (procedure 1) are characterized by a large scatter in the average particle size: from 30 μm (brushite/monetite/TCP) to 220 (TCP) and 350 μm (HA). Note that, in the case of spontaneous dispersion, the size of individual granules reaches 2.3 mm (Fig. 2a). The granule size distribution can be represented by a lognormal law with fitting reliability (R^2) of 0.984–0.989. The brushite/monetite/TCP granules have a narrow particle size distribution, in the range 16–80 μm , whereas the granules consisting of the neutral and basic calcium phosphates have a broad particle size distribution: from 75 μm to 2.3 mm for the HA and from 80 to 920 μm for the TCP. Therefore, the granules based on the acid calcium phosphates are homogeneous, in contrast to the polydisperse granules of the neutral and basic calcium phosphates, which are typically subject to aggregation processes during drying.

The calcium phosphate granules have a significantly inhomogeneous morphology. In particular, the surface layer of the TCP granules consists of inter-

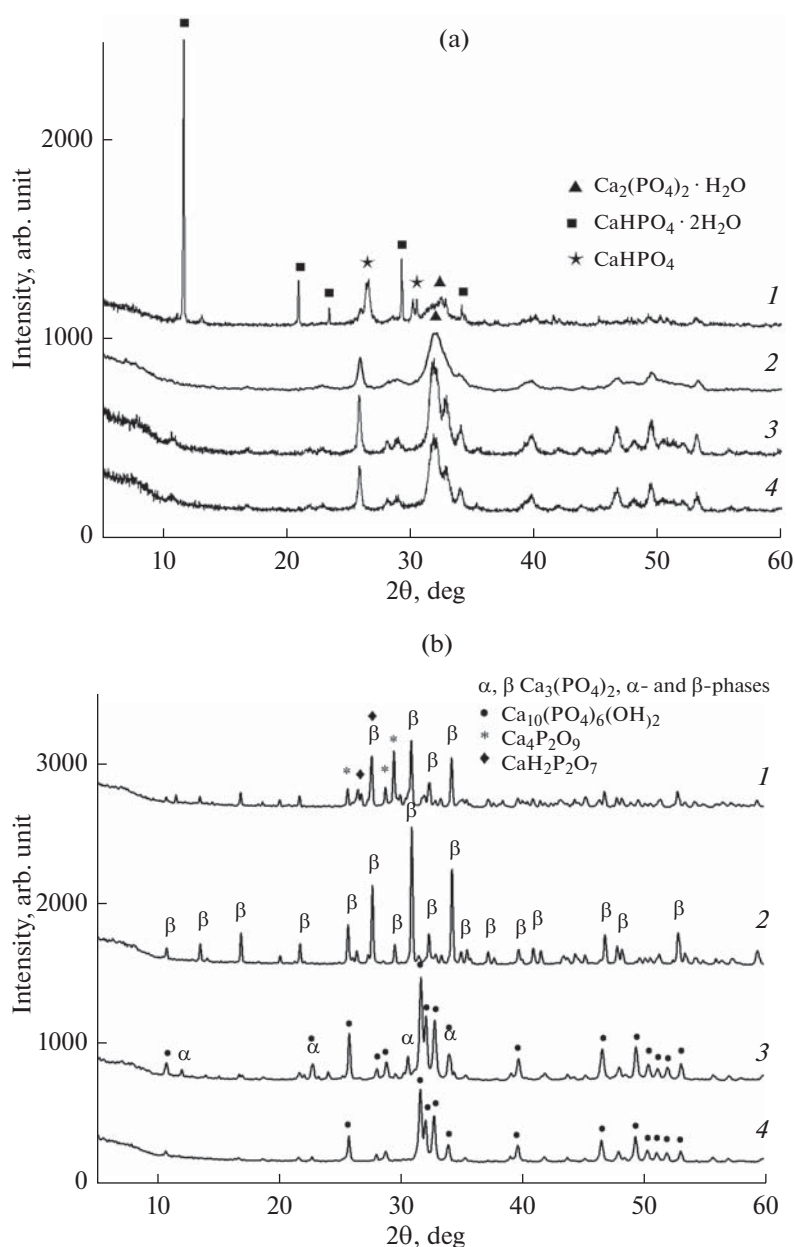


Fig. 1. X-ray diffraction patterns of the calcium phosphates (a) dried at 60–70°C and (b) heat-treated at 800°C: (1) Ca : P = 1.5, pH 5–6; (2) Ca : P = 1.5, pH 6–8; (3) Ca : P = 1.67, pH 8–9; (4) Ca : P = 1.67, pH 10–11.

grown spherical particles, with 0.5- to 1- μm -diameter macropores in between (Fig. 2b).

The obtained granules have a rather large specific surface area ($A_{\text{BET}} = 45\text{--}155\text{ m}^2/\text{g}$), adsorption pore volume of up to $0.5\text{ cm}^3/\text{g}$, and mesopore size in the range 11–18 nm (Table 1). The HA granules have the largest specific surface area, which may be due to the presence of a porous structure formed through the aggregation of the HA nanoparticles, as shown previously [8, 10, 13]. The smaller specific surface area of the acid calcium phosphate granules can probably be

understood in terms of the morphological features of their crystals: brushite and monetite typically consist of large plates, whereas HA and TCP usually have the form of spherical particles capable of spontaneous agglomeration. It is worth noting that high-temperature heat treatment of calcium phosphates markedly degrades their structural and adsorption characteristics. In particular, after heat treatment at 800°C HA has a relatively small specific surface area ($A_{\text{BET}} = 17\text{ m}^2/\text{g}$).

Analysis of nitrogen physisorption data indicates that the HA and TCP granules are mesoporous and

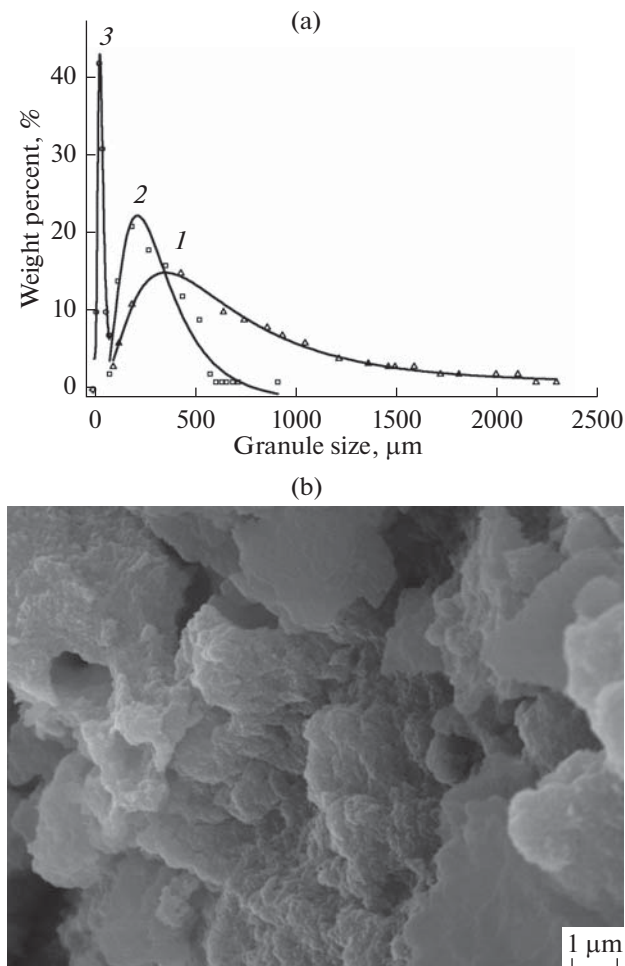


Fig. 2. (a) Size distributions of the granules prepared by the cryogenic processing of the 3 to 5% calcium phosphate gels (procedure 1) and (b) electron micrograph of the surface of the TCP granules: (1) HA, (2) TCP, (3) brushite/monetite/TCP. The open symbols represent the experimental data and the solid lines represent the best fit lognormal distributions.

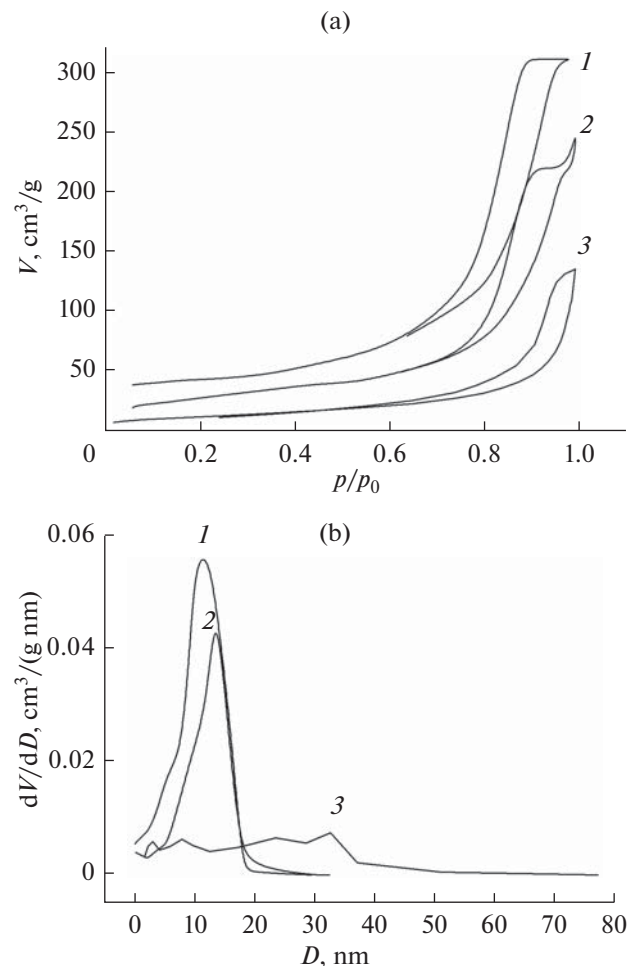


Fig. 3. (a) Low-temperature nitrogen adsorption–desorption isotherms and (b) adsorption pore volume distributions of the calcium phosphate granules prepared by the cryogenic processing of the 3 to 5% calcium phosphate gels (procedure 1): (1) HA, (2) TCP, (3) brushite/monetite/TCP.

have adsorption isotherms in the form of narrow hysteresis loops (Fig. 3a). The largest mesopore volume (0.055 cm³/(g nm)) is offered by the HA granules (Fig. 3b). Raising the concentration of the acid calcium phosphates leads to a decrease in the maximum pore volume to 0.042 cm³/(g nm) (TCP) and 0.07 cm³/(g nm) (brushite/monetite/TCP), which correlates with the

small specific surface area of these granules compared to the HA granules.

The formation of mesoporous granules from the calcium phosphate gels may be due to changes in the physicochemical properties of free and bound water as it passes from one state of aggregation to another. This is accompanied by hydrogen bond breaking and disin-

Table 1. Structural and adsorption properties of the calcium phosphate granules produced using a 3 to 5% calcium phosphate gel (procedure 1)

Phase composition	A_{BET} , m ² /g	$V_{\text{sp ads}}$, cm ³ /g	$V_{\text{BJH ads}}$, cm ³ /g	$V_{\text{BJH des}}$, cm ³ /g	$D_{\text{BJH ads}}$, nm	$D_{\text{BJH des}}$, nm
HA	155	0.487	0.493	0.491	11	10
β- TCP	100	0.338	0.393	0.390	16	13
Brushite/monetite/TCP	45	0.0001	0.212	0.211	18	14

tegration of the connected gel structure, leading to the formation of irregularly shaped mesoporous calcium phosphate granules.

In procedure 2, granules were prepared by extruding HA/ α -TCP paste. After air-drying, the average granule size ranged from 500 μm to 1.5 mm. The granules prepared using cryogenic processing have a narrow particle size distribution, with an average size of 650 μm . The granules produced via treatment with hydrogen peroxide have a broad size distribution, and some of them reach 4 mm in size as a result of mechanical adhesion during drying. The granule size distribution is well represented by a lognormal law ($R^2 = 0.97\text{--}0.98$) (Fig. 4). Surface processing of the HA/ α -TCP granules with an HA suspension (aqueous or based on a 1% PVA solution) makes it possible to obtain granules uniform in size: the size of the small granules increases twofold, reaching 200 μm , whereas the size of the large granules remains essentially unchanged (Fig. 4).

The surface morphology of the calcium phosphate granules prepared by procedure 2 (extrusion) is characterized by an inhomogeneous pore structure and is formed by intergrown agglomerates of spherical particles (Fig. 5). After air-drying, the average size of individual particles is 0.1 μm (Fig. 5a); after cryogenic processing, we observe aggregates of particles up to 0.2–0.5 μm in size (Fig. 5b). Treatment with hydrogen peroxide leads to marked coalescence of particle aggregates and the formation of rather large macropores, reaching 0.5 μm in size (Fig. 5c).

According to the IUPAC classification [14], the calcium phosphate granules have type V adsorption isotherms (Fig. 6a), characteristic of porous adsorbents with a weak adsorbent–adsorbate interaction. Such isotherms are rarely encountered. They are concave upward relative to the p/p_0 axis throughout their extension and are a variety of type III in the presence of mesopores. According to the capillary condensation hysteresis, the isotherms can be ascribed to type H1, characteristic of agglomerates of spherical particles uniform in size and packing density.

The HA/ α -TCP granules prepared through extrusion (procedure 2) have a smaller specific surface area than do the phase-pure HA and β -TCP granules (procedure 1) (Tables 1, 2). Characteristically, additional cryogenic processing or treatment of moist HA/ α -TCP granules with hydrogen peroxide contributes to a marked increase in specific surface area. The average mesopore diameter is 13–14 nm and the adsorption pore volume ranges from 0.050 to 0.069 $\text{cm}^3/(\text{g nm})$ (Fig. 6b).

The adsorption volume and mesopore diameter of the samples do not correlate with their specific surface area. It is, therefore, reasonable to assume that a con-

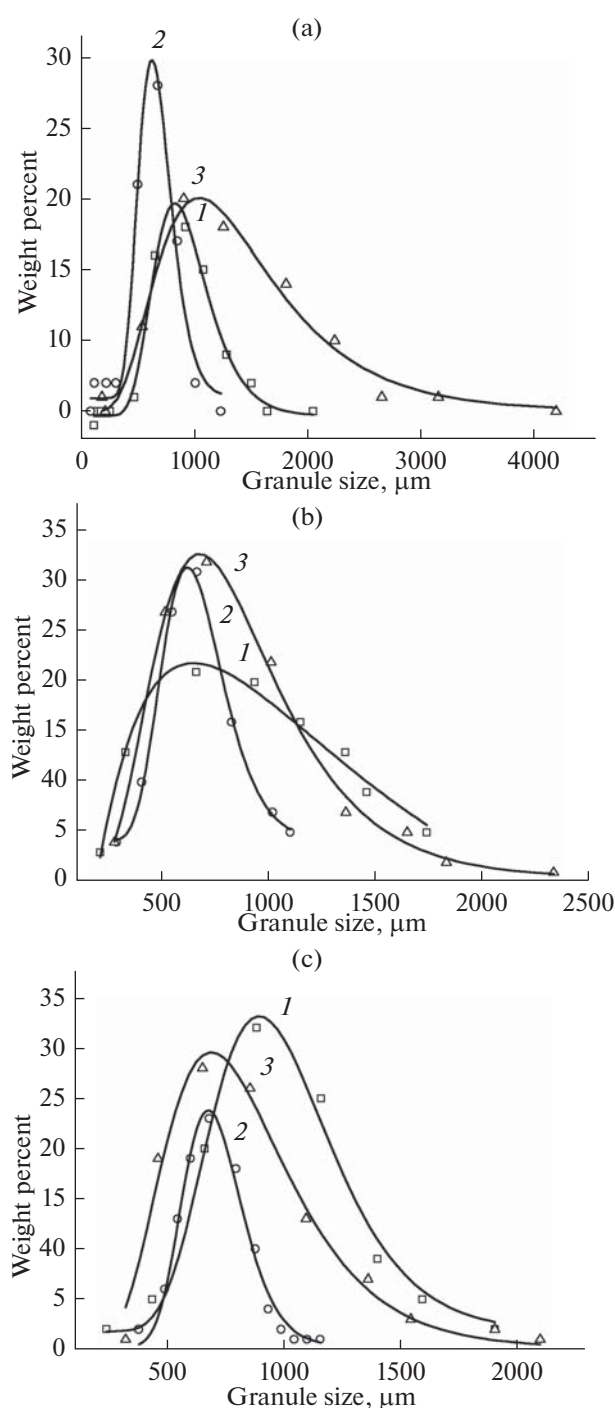


Fig. 4. Size distributions of the (a) uncoated, (b) HA-coated, and (c) HA/PVA-coated HA/ α -TCP granules prepared by procedure 2: (1) air-drying, (2) cryogenic processing, (3) treatment with H_2O_2 . The open symbols represent the experimental data and the solid lines represent the best fit lognormal distributions.

siderable contribution to the active surface area is made by not only mesopores but also macropores. It is worth noting that coating HA/ α -TCP granules with an HA or HA/PVA layer increases their specific surface

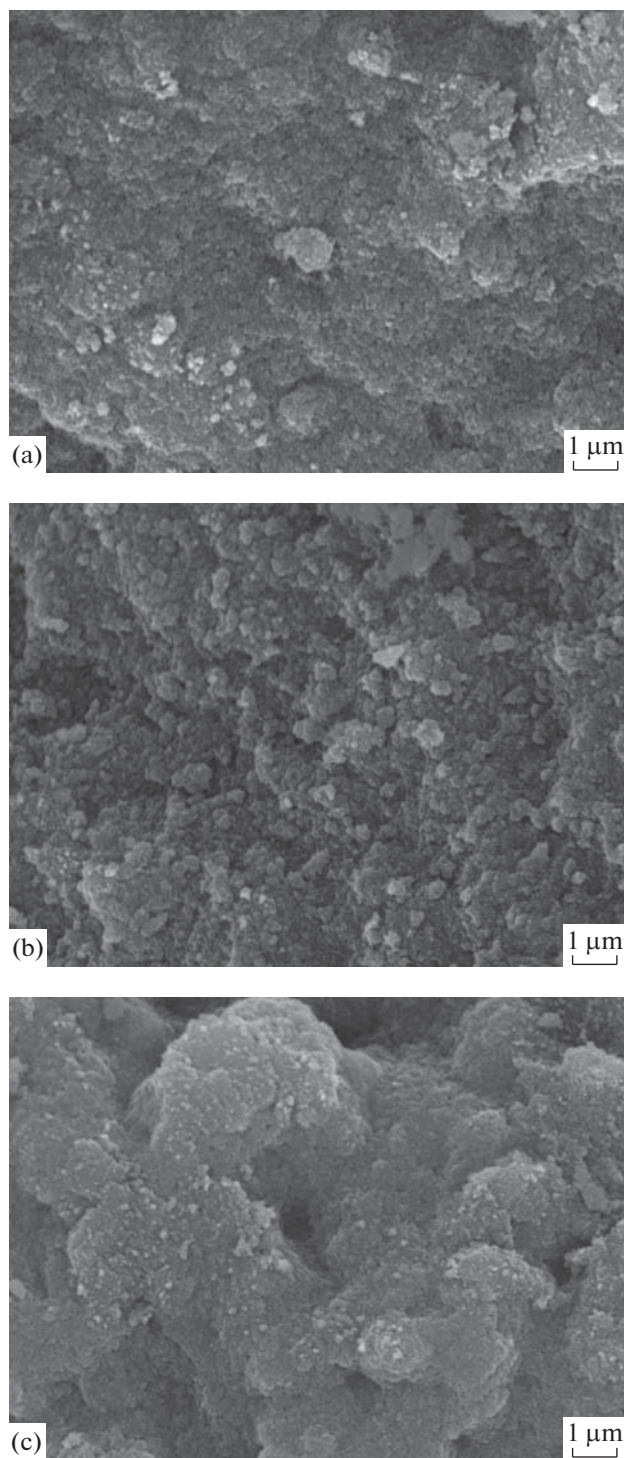


Fig. 5. Electron micrograph of the surface of the HA/ α -TCP granules (procedure 2): (a) air-drying, (b) cryogenic processing, (c) treatment with H_2O_2 .

area only in the case of the granules with initially poorer structural and adsorption characteristics.

Preclinical trials in which titanium implants with HA/ α -TCP granules were inserted in a model defect

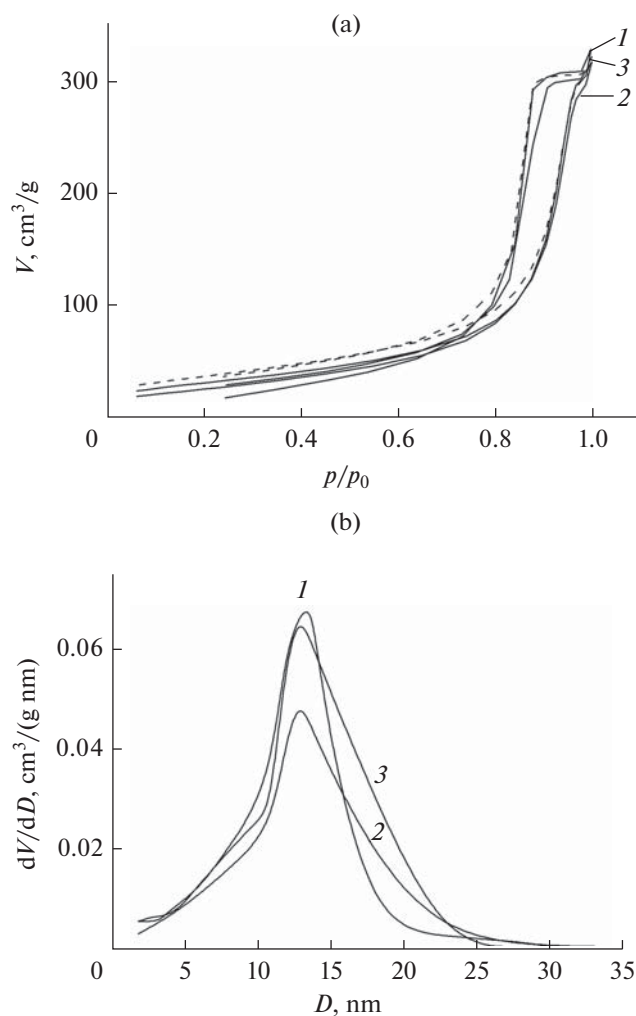


Fig. 6. (a) Low-temperature nitrogen adsorption–desorption isotherms and (b) adsorption pore volume distributions of the calcium phosphate granules prepared by procedure 2: (1) drying at 20°C , (2) cryogenic processing at -18°C , (3) treatment with H_2O_2 .

in the parietal bone of rats showed that, three months after the surgical intervention, there was a tighter contact between the implant and bone tissue in the animals of group III, with calcium phosphate granules. A morphological examination indicated that the region of the bone tissue defect between the inserted implant and parent bed contained tissue formed by young bone trabeculae with osteoblasts on their surface. The intertrabecular spaces were characterized by high cellularity and vascularization. In the peripheral parts of the implant insertion region, osteogenesis was due to young bone trabeculae growing into the parent bed, with osteoblasts located at their edges. In the case of the use of calcium phosphate granules, we visually observed high cellularity in the red bone marrow region compared to other groups.

Table 2. Structural and adsorption properties of the calcium phosphate granules produced using HA/ α -TCP paste (procedure 2)

Composition	Preparation conditions	A_{BET} , m ² /g	$V_{\text{sp ads}}$, cm ³ /g	$V_{\text{BJH ads}}$, cm ³ /g	$V_{\text{BJH des}}$, cm ³ /g	$D_{\text{BJH ads}}$, nm	$D_{\text{BJH des}}$, nm
HA/ α -TCP	20°C	84	0.468	0.506	0.505	15	11
(HA/ α -TCP)/HA		115	0.466	0.515	0.513	16	12
(HA/ α -TCP)/(HA/PVA)		111	0.436	0.472	0.470	16	12
HA/ α -TCP	−18°C	103	0.456	0.490	0.488	15	12
(HA/ α -TCP)/HA		104	0.494	0.541	0.539	19	19
(HA/ α -TCP)/(HA/PVA)		102	0.468	0.509	0.508	16	12
HA/ α -TCP	H ₂ O ₂	123	0.469	0.499	0.496	14	11
(HA/ α -TCP)/HA		113	0.462	0.500	0.498	15	12
(HA/ α -TCP)/(HA/PVA)		100	0.431	0.467	0.465	16	12

CONCLUSIONS

Mesoporous calcium phosphate granules have been prepared using cryogenic processing (−18°C) of 3 to 5% calcium phosphate (HA, β -TCP, and brushite/monetite/TCP) gels and extrusion of a 28 to 31% HA/ α -TCP paste. The brushite/monetite/TCP granules are homogeneous, with an average size of 30 μm . The calcium phosphate granules based on neutral and basic calcium phosphates are polydisperse, with an average granule size of 220 (TCP) or 350 μm (HA). According to low-temperature nitrogen physisorption–desorption data, the granules have type V sorption isotherms. The largest specific surface area ($A_{\text{BET}} = 155 \text{ m}^2/\text{g}$) is offered by the HA granules prepared via the cryogenic processing of gel at −18°C. The addition of acid calcium phosphates leads to a reduction in the specific surface area of the granules to 45 m^2/g . Surface processing of the HA/ α -TCP granules with a 5% HA suspension leads to an increase in their specific surface area from 84 to 115 m^2/g . Scanning electron microscopy results demonstrate that the surface layer of the calcium phosphate granules consists of spherical agglomerates. Preclinical in vivo trials on rats show that inserting calcium phosphate granules in a model bone defect accelerates reparative osteogenesis processes in the damaged bone tissue.

ACKNOWLEDGMENTS

This work was supported by the Belarusian Academy of Sciences (national research program °Chemical Technologies and Materials, subprogram no. 2.1) and the World Federation of Scientists (2016–2017).

REFERENCES

1. Pavlenko, A.V., Tokarskii, V.F., Prots', G.B., Kliment'ev, V.G., and Shterenberg, A., Easy-graft®CRYSTAL, a novel, β -tricalcium phosphate-based biphasic bone substitute material for bone defects, *Sovrem. Stomatol.*, 2013, no. 1, pp. 89–92.
2. Daculsi, G., Uzel, A.P., Weiss, P., Goyenvalle, E., and Aguado, E., Developments in injectable multiphasic biomaterials. the performance of microporous biphasic calcium phosphate granules and hydrogels, *J. Mater. Sci.: Mater. Med.*, 2010, vol. 21, pp. 855–861.
3. Le Guehennec, L., Goyenvalle, E., Aguado, E., Pilet, P., Bagot D'Arc, M., Bilban, M., Spaethe, R., and Daculsi, G., MBCP biphasic calcium phosphate granules and tissucol fibrin sealant in rabbit femoral defects: the effect of fibrin on bone ingrowth, *J. Mater. Sci.: Mater. Med.*, 2005, vol. 16, pp. 29–35.
4. Le Nihouannen, D., Le Guehennec, L., Rouillon, Th., Pilet, P., Bilban, M., Layrollea, P., and Daculsi, G., Micro-architecture of calcium phosphate granules and fibrin glue composites for bone tissue engineering, *Biomaterials*, 2006, vol. 27, pp. 2716–2722.
5. Daculsi, G., LeGeros, R.Z., Heughebaert, M., and Barbieux, I., Formation of carbonate-apatite crystals after implantation of calcium phosphate ceramics, *Calcif. Tissue. Int.*, 1990, vol. 46, pp. 20–27.
6. Barinov, S.M. and Komlev, V.S., *Biokeramika na osnove fosfatov kal'tsiya (Calcium Phosphate-Based Bioceramics)*, Moscow: Nauka, 2005.
7. Musskaya, O.N., Kulak, A.I., Lesnikovich, L.A., Butovskaya, G.V., Ulasevich, S.A., Krut'ko, V.K., and Sycheva, O.A., Hydroxyapatite xerogel dehydration kinetics under nonisothermal conditions, *Zh. Obshch. Khim.*, 2012, vol. 82, no. 8, pp. 1258–1262.
8. Musskaya, O.N., Kulak, A.I., Krut'ko, V.K., Lesnikovich, L.A., and Kovalenko, A.Yu., Bioactive hydroxyap-

- atite xerogel, *Vestsi Nats. Akad. Navuk Belarusi, Ser. Khim. Navuk*, 2011, no. 1, pp. 5–11.
9. Shchegrov, L.N., *Fosfaty dvukhvalentnykh metallov (Divalent Metal Phosphates)*, Kiev: Naukova Dumka, 1987.
 10. Krut'ko, V.K., Kulak, A.I., Lesnikovich, L.A., Trofimova, I.V., Musskaya, O.N., Zhavnerko, G.K., and Paribok, I.V., Influence of the dehydration procedure on the physicochemical properties of nanocrystalline hydroxylapatite xerogel, *Russ. J. Gen. Chem.*, 2007, vol. 77, no. 3, pp. 336–342.
 11. Ulasevich, S.A., Krut'ko, V.K., Musskaya, O.N., Kulak, A.I., Lesnikovich, L.A., and Safronova, T.V., Influence of maturation conditions of hydroxyapatite gel on the composition of xerogel, *Russ. J. Appl. Chem.*, 2013, vol. 86, no. 2, pp. 146–150.
 12. Ulasevich, S.A., Kulak, A.I., Krut'ko, V.K., Musskaya, O.N., Lesnikovich, L.A., and Safronova, T.V., Hydroxyapatite formation under combined treatment of a gel in the secondary maturation stage, *Russ. J. Gen. Chem.*, 2015, vol. 85, no. 1, pp. 1–6.
 13. Musskaya, O.N., Kulak, A.I., Krut'ko, V.K., Lesnikovich, L.A., and Ulasevich, S.A., Dehydration of hydroxyapatite and tricalcium phosphate gels to bioactive xerogels, *Sviridovskie Chteniya*, 2010, no. 6, pp. 41–48.
 14. Sing, K.S.W., Everett, D.H., Haul, R.A.W., Moscou, L., Pierotti, R.A., Rouquerol, J., and Siemieniewska, T., Reporting physisorption data for gas/solid systems with special reference to the determination of surface area and porosity, *Pure Appl. Chem.*, 1985, vol. 57, no. 4, pp. 603–619.

Translated by O. Tsarev

SPELL: 1. OK